Age-specific Topology Minimization in a One-dimensional Model Describing Carotid Haemodynamics

Irene Suriani[1], Sabina Manzari[3], R. Arthur Bouwman[2], Massimo Mischi[1], Kevin D. Lau[3]

[1]Eindhoven University of Technology, Eindhoven, Netherlands
[2]Catharina Hospital, Eindhoven, Netherlands
[3]Philips Research, Eindhoven, Netherlands

Abstract

Patient-specific one-dimensional (1D) haemodynamic models can support personalized clinical decisions through an improved interpretation of carotid ultrasound (cUS) velocity and diameter waveforms. However, personalized 1D models of the arterial vasculature require the estimation of a large number of parameters from in-vivo measurements, some often not readily available in most clinical settings. In such cases, we are confronted with a problem of complexity optimization: what is the minimum required 1D topology (i.e., the number of 1D arterial branches included in the model network) such that the least possible number of parameters are to be assumed, while still being able to accurately capture characteristic cUS waveform features?

In this work, using a systematic method for 1D model reduction, we have shown that the minimum topology required to accurately simulate cUS waveforms varies in virtual subjects of different ages. Using this approach, we have selected age-specific reduced models that retain carotid waveform features with NRMSE <4% for velocity and <0.15% for diameter.

Finally, we have used wave power analysis (WPA) to elucidate the location of origin of reflected waves responsible for cUS waveform features, and investigated the effect of model reduction on these.

1. Introduction

The analysis of cUS velocity and diameter waveforms provides information about individual cardiovascular health (e.g., vascular ageing, haemodynamic status) [1], [2]. Such waveforms can be simulated using patient-specific 1D haemodynamic models, which are parameterized based on individual in-vivo measurements [3]. These models can facilitate the interpretation of cUS waveforms and improve cUS-based personalized clinical decision support.

1D models of the arterial system may include up to thousands of arteries [4], [5]. In such cases, models are typically parameterized using population data available from the literature, and are meant to represent an 'average subject'. However, to build such models on a patient-specific basis is unfeasible, as this would require an unrealistic number of in-vivo measurements (e.g. length, diameter, and compliance of each vessel). For practical applications, models should only rely on readily available clinical data. For models built upon typical clinical data, it is thus necessary to determine the lowest level of topological complexity required to accurately simulate cUS waveforms, without loss of features of interest.

In this work, we investigated whether such a minimum required topology is age-specific, using a 1D modelling-based virtual population (VP) of subjects aged 20 to 80 years old [6]. For each age decade-specific subject, we used an algebraic method proposed by Epstein to create consistently reduced models by progressively lumping 1D segments into equivalent 0D RCR Windkessel (RCR-WK) terminal elements [7].

Finally, we used WPA to identify the locations, along the arterial network, where reflected waves responsible for characteristic cUS waveform features originate. We furthermore investigated how forward and backward travelling waves change in reduced models, to elucidate the reasons behind the loss of accuracy seen with topology reduction.

2. Methods

2.1. The baseline model and ageing virtual population

This work is based on a 1D modelling approach, wherein equations describing fluid dynamics through compliant vessels are solved throughout the arterial network to obtain instantaneous pressure, vessel luminal area, cross-sectional mean velocity, and flow [8]. At the inlet of the model, a realistic aortic flow waveform is prescribed, and at the terminal branches, RCR-WK elements are connected, to account for peripheral resistance, compliance, and reflections [8]. In this work, equations were solved by means of a Discontinuous Galerkin finite element scheme, with time integration via the explicit second-order Adam-Bashforth method. Time

stepping was performed at 0.01 ms, and 15 seconds were simulated to ensure convergence. This was implemented using the NEKTAR++ Pulse Wave Solver [9].

We started with a validated 55-branch topology (the 'complete' in Fig.1), able to accurately reproduce all characteristic cUS waveform features (e.g., foot, systolic and secondary systolic peaks, dicrotic notch of the velocity waveform, see Fig.2). We used a VP wherein ageing was simulated by scaling cardiovascular parameters according to documented in-vivo age-variations, and verifying that simulated age-related changes in cUS waveform features follow in-vivo population trends correctly [10].

2.2. Model reduction

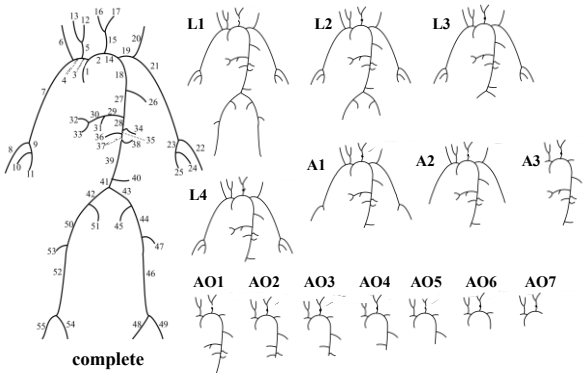

Figure 1: Complete and reduced topologies considered.

To obtain the minimal required topology for each age group, we progressively reduced the number of 1D segments included in each of our virtual subjects, analysing the accuracy of resulting cUS waveforms at each reduction step. We used the methodology by Epstein et al. to collapse 1D branches into RCR-WK elements [7]. Briefly, equivalent lumped resistance R_{eq} and compliance C_{eq} are obtained for each truncated 1D segment as:

$$R_{eq} = 2(\xi + 2)\pi\mu \int_0^l \frac{1}{A_d^2} dx, \quad (1)$$

$$C_{eq} = \frac{1}{\varrho} \int_0^l \frac{A_d}{c_d^2} dx, \quad (2)$$

with ξ=9 velocity profile polynomial, A_d diastolic area, c_d diastolic wavespeed, l vessel length, μ=2 mPA·s blood viscosity, and ρ=1060 kg/m^3 blood density.

Starting from the complete 55-branch topology, we first truncated arteries in the legs (in Fig.1, L1 to L4), then in the arms (A1 to A3), then proceeded with aortic and abdominal vessels (AO1 to AO7). The impact of each reduction step on the simulated cUS waveforms (extracted at the midpoint of the left common carotid, i.e., segment 15 in Fig.1) was quantified through the following error metrics with respect to the waveforms simulated using the complete model:

- normalized root-mean-square error (NRMSE) of the velocity and diameter waveforms,
- absolute errors of the main characteristic landmarks of both waveforms: foot, systolic and secondary systolic peaks, and dicrotic notch for velocity (Fig. 2); systolic, diastolic, and mean diameter.

A threshold of 4% velocity NRMSE, and of 1 cm/s on the absolute value errors of all velocity landmarks were used to discern the minimum required topology for each age group.

2.3. Wave Power Analysis

WPA allows to quantify the power of forward and backward waves travelling through a given arterial cross section. Positive (wp+) and negative power (wp–) are measured in Watts and obtained as follows:

$$wp\pm = \pm\frac{1}{4Z_c}(dP \pm Z_c dQ)^2 \quad (3)$$

where dP and dQ are incremental changes in pressure and flow, and $Z_c = \rho c/A$ the vessel's characteristic impedance, a function of blood density (ρ), wave speed (c), and area (A) [11].

We obtained wp± at the proximal, midpoint, and distal location of every aortic segment, and of the left common carotid. By comparing the synchronous time-domain WPA graphs obtained at each location, the anatomical origin of the backward travelling waves responsible for specific carotid waveform features was located.

3. Results

3.1. An age-specific minimal 1D topology

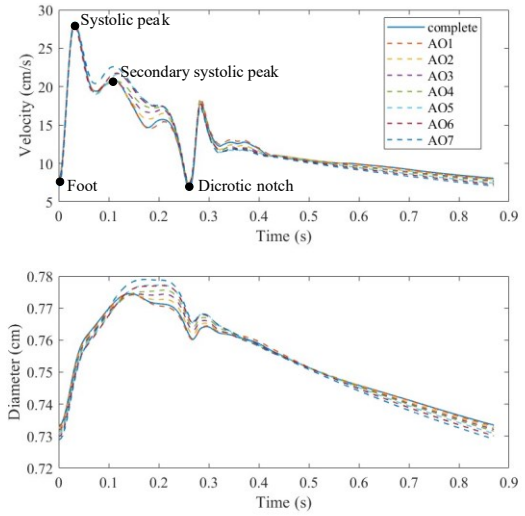

Figure 2: Velocity and diameter waveforms at different levels of aortic reduction for a 35-year-old subject.

For all age-specific subjects, the error metrics described in Section 2.2 were calculated for each reduction step (L1 to AO7, see Fig. 1). Fig. 2 shows the simulated cUS waveforms resulting from the complete model and from

reduction steps AO1 to AO7 in an adult virtual subject.

Considering the 4% velocity NRMSE threshold, the resulting minimum topology was found to be age-specific: AO2 for subjects aged <50 years old, AO1 for older subjects (absolute errors were well below 1 cm/s in both cases). Diameter NRMSE was <0.15%, and absolute value errors <0.02 mm. By adopting the two age-specific minimum topologies, the number of 1D branches was reduced from 55 to 20 for the younger group, and 24 for the elderly group. The number of required input parameters decreased from 359 to 177 and 151 respectively.

3.2. Observed wave reflection patterns in the complete and reduced models

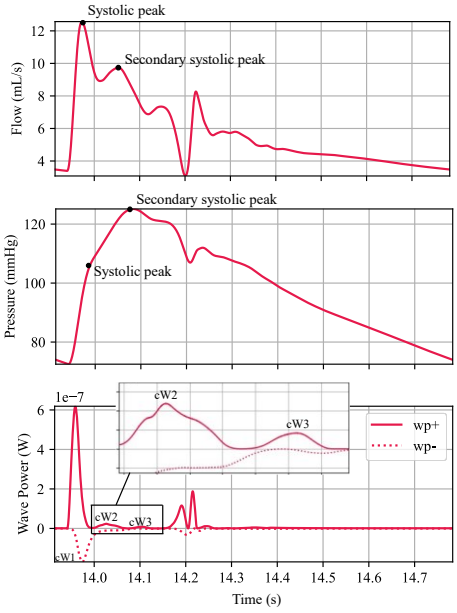

Figure 3: WPA at the midpoint of the common carotid artery in a 35-year-old subject.

Fig. 3 shows pressure, flow and the resulting wp± at the midpoint of the left common carotid. We have identified three reflected waves that appear to contribute to the characteristic morphology of the carotid waveform: cW1, a reflected wave travelling back from the carotid bifurcation, which decelerates flow and augments pressure following the first systolic peak, cW2, and cW3, two small forward waves contributing, respectively, to the secondary systolic peak, and to the subsequent part of systole until the dicrotic notch. By observing the timing and presence of backward reflected waves along the aortic pathway, we identified the origins of waves cW2 and cW3 in the aorta, here denoted as aW2 and aW3. Namely, aW2 appears as a reflection at the interface between abdominal aorta and left renal artery (Fig. 4 A), segments 35 and 36 in Fig. 1, and propagates back until it enters the carotid, becoming forward wave cW2. Similarly, aW3 is formed at the distal end of the abdominal aorta (segment 41 in Fig. 1) at the iliac bifurcation. As we can see in Fig. 4 B, in the reduced AO1 or AO2 topologies, aW3 originates earlier in time.

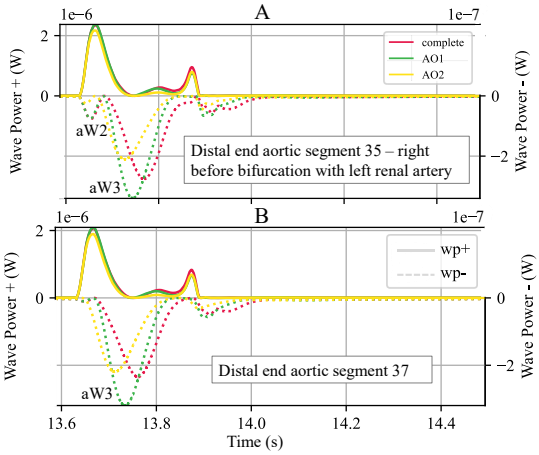

Figure 4: WPA of a 75-year-old subject comparing the complete and AO1, AO2 reduction levels. A – distal end of aortic segment 35 (see Fig. 1); B – distal end of aortic segment 37 (see Fig. 1).

As evident from Fig. 5, in younger subjects, backward-travelling waves are weaker relative to the forward waves as compared to elderly subjects. For instance, in a 25-year-old, the peak power of backward travelling waves through the abdominal aorta reaches only 7% of the peak power of concurrent forward travelling waves, while in a 75-year-old, the peak backward power is approximately 17% of the peak forward power.

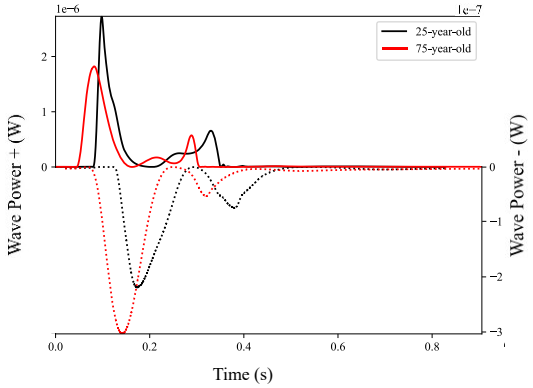

Figure 5: wp± through the abdominal aorta for a young and an elderly subject (complete model). Positive and negative y axes are scaled differently (scales indicated on top-left and top-right, respectively).

4. Discussion

We have applied the same topological reduction procedure to virtual subjects belonging to different age decades, and have found that the effect of model reduction

on the accuracy of simulated cUS waveforms varies with age. Errors increase faster with the number of removed branches in the elderly than in young, thus two different minimum topologies have been selected depending on age: AO2 for subjects <50 years old, AO1 for those above 50.

As can be observed in Fig. 2, reduction-caused abnormalities in simulated cUS waveforms occur mainly during the second half of the systolic interval, after the secondary systolic peak up until the dicrotic notch. Via WPA, it emerged that this part of the waveform is strongly affected by the reflected wave aW3, which originates, in the complete model, at the iliac bifurcation and travels backwards into the carotid (here becoming a forward wave cW3). When aortic segments are truncated, aW3 is generated earlier in time and more proximally in the aorta because of the truncation of aortic segments. This allows cW3 to occur earlier at the level of the carotid, injecting wave power earlier during the pressure and flow decay after the secondary systolic peak, thus generating a peak (or plateau) at a higher flow and pressure. This effect is more noticeable in elderly subjects, because their reflected waves are stronger than in younger subjects (17% vs 7% of peak forward power). Thus, the need for a more detailed topology in elderly subjects.

Conversely, the secondary systolic peak in the carotid waveform is affected by cW2, a reflected wave originating at the aortic bifurcation with the left renal artery. Therefore, models should include at least this bifurcation if they are to maintain an accurate prediction of this waveform feature. As shown in Fig. 6, WPA at the first segment of the abdominal aorta (35 in Fig. 1) of AO3, a reduced topology wherein the bifurcation with left renal artery is truncated, does not contain the two peaks aW2 and aW3, as does the complete one, and instead includes an earlier reflection aW3*, resulting in a distortion of the carotid waveform.

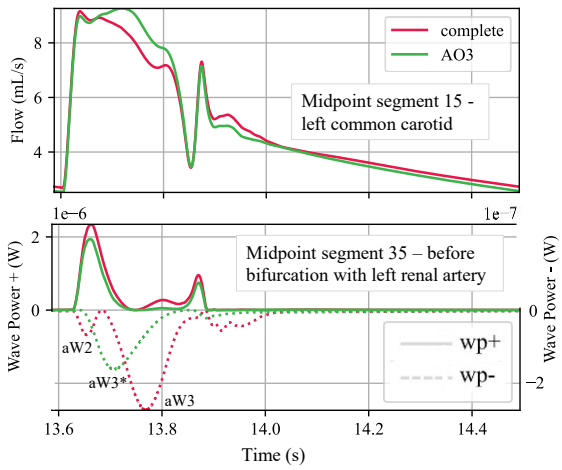

Figure 6: Flow waveform and WPA of the 75-year-old complete model versus AO3, a model where the bifurcation responsible for aW2 is truncated.

5. Conclusions

Starting from a 55-branch 1D model, we have performed a systematic 1D-to-0D reduction in virtual subjects of different ages from 20 to 80 years old. We have found that the minimum 1D topology required to accurately simulate cUS waveforms is age-specific: based on a 4% velocity NRMSE threshold, a 20-branch topology for subjects younger than 50 years old, and a 24-branch topology for those older. With these, the initial set of input model parameters is reduced by more than half.

Finally, using WPA we have identified the location of origin of reflected waves contributing to carotid waveform morphology: aortic-left renal and aortic-iliac bifurcations. Model reduction affects the presence and/or timing of these reflected waves, distorting the resulting carotid waveform, especially in elderly subjects wherein reflected waves play a greater role.

References

[1] K. Hirata, et al., "Age-Related Changes in Carotid Artery Flow and Pressure Pulses. Possible Implications for Cerebral Microvascular Disease," *Stroke*, pp. 2552–2556, 2006.

[2] L. Beier, et al., "Carotid Ultrasound to Predict Fluid Responsiveness," *J. Ultrasound Med.*, vol. 39, no. 10, pp. 1965–1976, 2020.

[3] J. Alastruey, et al., "On the impact of modelling assumptions in multi-scale, subject-specific models of aortic haemodynamics," *J. R. Soc. Interface*, vol. 13, no. 119, 2016.

[4] P. J. Blanco, et al., "An anatomically detailed arterial network model for one-dimensional computational hemodynamics," *IEEE Trans. Biomed. Eng.*, vol. 62, no. 2, pp. 736–753, 2015.

[5] P. Perdikaris, et al., "An effective fractal-tree closure model for simulating blood flow in large arterial networks", *Ann. Biomed. Eng.*, vol. 43, no. 6, pp. 1432–1442, 2015.

[6] I. Suriani, et al., "Development, Validation and Uses of an Age-Specific Virtual Population for the Study of Carotid Haemodynamics," *Manuscript in Preparation*.

[7] S. Epstein, et al., "Reducing the number of parameters in 1D arterial blood flow modeling: Less is more for patient-specific simulations," *Am. J. Physiol. - Hear. Circ. Physiol.*, vol. 309, no. 1, pp. H222–H234, 2015.

[8] J. Alastruey, et al., "Arterial pulse wave haemodynamics," in *11th International Conference on Pressure Surges*, 2012, pp. 401–443.

[9] S. Sherwin and M. Kirby, "Nektar++ Spectral/hp Element Framework." https://www.nektar.info/

[10] I. Suriani, et al., "Validation of an aging virtual population for the study of carotid hemodynamics," *Annu. Int. Conf. IEEE Eng. Med. Biol. Soc.*, pp. 4249–4252, 2021.

[11] J. P. Mynard, et al., "Measurement, Analysis and Interpretation of Pressure/Flow Waves in Blood Vessels," *Front. Physiol.*, vol. 11, no. August, pp. 1–26, 2020.

Address for correspondence:

Irene Suriani
Groene Loper 19, 5612AP, Eindhoven, The Netherlands
i.suriani@tue.nl